Pflugers Arch - Eur J Physiol (2011) 462:495–504
DOI 10.1007/s00424-011-0989-3

CARDIOVASCULAR PHYSIOLOGY

Refractory dispersion promotes conduction disturbance and arrhythmias in a *Scn5a*$^{+/-}$ mouse model

Claire A. Martin · Andrew A. Grace · Christopher L.-H. Huang

Received: 18 April 2011 / Revised: 10 June 2011 / Accepted: 15 June 2011 / Published online: 21 July 2011
© The Author(s) 2011. This article is published with open access at Springerlink.com

Abstract Accentuated right ventricular (RV) gradients in action potential duration (APD) have been implicated in the arrhythmogenicity observed in Brugada syndrome in studies assuming that ventricular effective refractory periods (VERPs) vary in concert with APDs. The present experiments use a genetically modified mouse model to explore spatial heterogeneities in VERP that in turn might affect conduction velocity, thereby causing arrhythmias. Activation latencies, APDs and VERPs recorded during programmed S1S2 protocols were compared in RV and left ventricular (LV) epicardia and endocardia of Langendorff-perfused wild-type (WT) and *Scn5a*$^{+/-}$ hearts. *Scn5a*$^{+/-}$ and WT hearts showed *similar* patterns of shorter VERPs in RV than LV epicardia, and in epicardia than endocardia. However, *Scn5a*$^{+/-}$ hearts showed *longer* VERPs, despite *shorter* APD_{90}s, than WT in all regions examined. The pro- and anti-arrhythmic agents flecainide and quinidine *increased* regional VERPs despite respectively *decreasing* and *increasing* the corresponding APD_{90}s particularly in *Scn5a*$^{+/-}$ RV epicardia. In contrast, *Scn5a*$^{+/-}$ hearts showed greater VERP gradients between neighbouring regions, particularly RV transmural gradients, than WT (9.1±1.1 vs. 5.7±0.5 ms, $p<0.05$, $n=12$). Flecainide *increased* (to 21± 0.9 ms, $p<0.05$, $n=6$) but quinidine *decreased* (to 4.5± 0.5 ms, $p<0.05$, $n=6$) these gradients, particularly across the *Scn5a*$^{+/-}$ RV. Finally, *Scn5a*$^{+/-}$ hearts showed greater conduction slowing than WT following S2 stimuli, particularly with flecainide administration. Rather than arrhythmogenesis resulting from increased transmural repolarization gradients in an early, phase 2, reentrant excitation mechanism, the present findings implicate RV VERP gradients in potential reentrant mechanisms involving impulse conduction slowed by partial refractoriness.

Keywords Cardiac electrophysiology · Ventricular fibrillation · Arrhythmia · Action potential · Sodium channel

C. A. Martin (✉) · C. L.-H. Huang
Physiological Laboratory, University of Cambridge,
Downing Site,
Cambridge CB2 3EG, UK
e-mail: clairemartin@gmail.com

A. A. Grace
Department of Biochemistry, University of Cambridge,
Downing Site,
Cambridge CB2 1QW, UK

Introduction

Brugada syndrome (BrS) is associated with decreased Na^+ channel function and increased incidences of polymorphic ventricular tachycardia (VT) and sudden cardiac death. Although genetically heterogeneous, up to 30% of patients have mutations in *SCN5A*, the only gene extensively studied in connection with BrS which encodes the cardiac Nav1.5 α-subunit [14]. Possible arrhythmogenic mechanisms were initially modelled using canine wedge preparations; these, however, entailed pharmacological manoeuvres with potentially nonspecific effects [51]. More recently, heterozygotic *Scn5a*$^{+/-}$ hearts, showing 50% reductions in their transmembrane Na^+ currents, have reproduced features of the human clinical condition, demonstrating ST elevation and enhanced arrhythmogenesis exacerbated by flecainide and relieved by quinidine [26].

Both canine and murine cardiac systems have demonstrated regions of shortened epicardial relative to endocardial action potential durations (APDs). In particular, murine *Scn5a*$^{+/-}$ hearts have demonstrated increased transmural APD gradients [27] and increased incidences of alternans,

particularly in the right ventricle (RV) [29], following flecainide administration. This localized AP shortening could potentially result in losses of the AP dome, thereby altering repolarization gradients within or across the myocardial wall. This could increase the likelihood of early epicardial 'phase II' re-excitation as a key arrhythmic mechanism in BrS. At the very least, such a mechanism could coexist with arrhythmic tendencies resulting from the altered conduction also expected from the loss of Na^+ channel function in BrS [30].

However, early reentry mechanisms would specifically require corresponding reductions in the epicardial refractory periods. Certainly, *normal* canine [12, 15] and human [22] hearts show closely related APDs and ventricular effective refractory periods (VERPs), with a recovery of excitability consistently occurring at ~85% repolarization over a wide range of steady-state cycle lengths. However, VERPs can be selectively affected by factors that need not similarly affect APD. These include the numbers, and time courses of activation or inactivation, of Na^+ and K^+ channels; the amplitude and duration of the applied stimuli [46]; and conditions of myocyte damage or ischaemia. Na^+ channel dysfunction therefore could well alter VERP differently from APD. Contrasting APD and VERP changes also occur under other arrhythmogenic circumstances, as in hypokalaemia [42]. Conflicting results concerning VERP durations in BrS have been reported in previous clinical studies [2] and experiments in cell expression lines (for references, see [6]).

However, systematic regional studies of VERPs have not hitherto been performed in either genetic or pharmacological BrS models. Thus, it has often implicitly been assumed that VERPs and APDs vary concordantly in both wild-type (WT) and BrS. However, murine *Scn5a*$^{+/-}$ hearts have been previously reported to show either similar [44] or greater [35] VERPs than WT hearts, depending on their specific arrhythmogenic properties. Both loss-of function Na^+ channel mutations and pharmacological Na^+ blocking agents such as flecainide and quinidine might be expected to increase VERP. If AP firing requires a critical number of Na^+ channels, a greater relative proportion would then be required to recover from refractoriness, and this would occur later in the repolarization phase.

The present experiments specifically assess the roles of VERPs and conduction latencies in arrhythmogenesis in *Scn5a*$^{+/-}$ hearts. They go on to compare these parameters in the RV and LV epicardium and endocardium following the introduction of flecainide or quinidine for the first time. These agents are used respectively to unmask ventricular arrhythmogenesis in otherwise asymptomatic BrS patients [7] and to achieve protective actions in symptomatic BrS [5]. VERP changes, whether by themselves or relative to those of APD, could well affect arrhythmogenicity, whether by altering AP recovery or affecting conduction characteristics. In the first case, arrhythmogenic mechanisms involving early, phase II, reentrant excitation, previously suggested for BrS [51], would require reductions in VERPs, at least in relation to APD. In the second, spatial differences in VERP, and the consequences of these for conduction, may remain critical to the initiation of reentrant arrhythmia in BrS. Clarifying such distinctions may be important to future work investigating possible pharmacological management for a condition for which current treatment primarily involves ICD implantation.

Materials and methods

Mice aged 4–8 months were obtained from breeding pairs of heterozygote *Scn5a*$^{+/-}$ and WT inbred 129/sv mice, initially supplied by Harlan (UK). The experiments used a Langendorff-perfused preparation adapted for the murine heart [4]. Perfusion of bicarbonate-buffered Krebs-Henseleit solution was maintained at a flow rate of 2–2.5 ml min^{-1} using a peristaltic pump (Watson-Marlow Bredel pumps model 505S, Falmouth, Cornwall, UK), and warmed and maintained at 37°C via a water jacket and circulator (Techne model C-85A, Cambridge, UK). Initial experiments using a thermometer probe placed on the epicardial or endocardial surfaces confirmed that a temperature of 37°C was reached in both regions. Where used, flecainide and quinidine (Sigma-Aldrich, Poole, UK) dissolved in buffer solution were perfused for 15 min prior to and throughout data acquisition at concentrations within the same range as known clinical therapeutic levels used in BrS (flecainide, 0.2–0.9 mg l^{-1}; quinidine, 1.0–3.0 mg l^{-1}) [38].

Monophasic action potentials (MAPs) were recorded using electrodes constructed from two pieces of galvanically chlorided, Teflon-coated, 0.25-mm diameter silver wire twisted together to form one contact electrode and one reference electrode. This was either placed against the cardiac surface for epicardial recordings or introduced into the ventricular cavity through a small access window created in the ventricular wall for endocardial recordings. Care was taken to avoid regional stretch by manipulation, especially at the thin RV wall. MAP signals were amplified and band-pass filtered between 0.1 and 300 Hz (Neurolog AC amplifiers and filters models NL104 and NL125/6, respectively; Digitimer, Welwyn Garden City, Herts, UK), then digitized using a 1401plus interface (Cambridge Electronic Design, Cambridge, Cambs., UK). Paired platinum stimulating electrodes were used to pace the heart.

Hearts underwent a programmed electrical stimulation (PES) technique of a 5-min period of 8-Hz regular pacing followed by cycles of a decremental paced electrogram

sequence comprising an eight-beat stimulus (S1) drive train at 8 Hz followed by an extra-stimulus (S2). The S1–S2 interval was reduced by 1 ms between successive drive trains until the preparation became either refractory or arrhythmic (Fig. 1a). The incidence of arrhythmogenesis was defined as the presence of VT lasting more than 1 s in any given trace. MAP waveforms were then analysed using Spike2 software (Cambridge Electronic Design). The point of maximum positive deflection was considered the point of 0% repolarization; that of full return to baseline of 100% repolarization. The APD during regular pacing was measured at 90% repolarization, APD_{90}, as shown in Fig. 1b. Activation latencies were calculated as the time from stimulus to the point of maximum positive deflection of the MAP waveform. L1 was defined as the activation latency following an S1 stimulus and L2 as the activation latency following the last S2 able to elicit an AP.

The VERP was also measured from the PES sequences. As explained in "Results," two independent measures of VERP were obtained. Firstly, VERP at the stimulus site was determined from the S1S2 interval at which the S2 stimulus last excited an action potential ($VERP_s$). Second, VERP at the recording site was determined from the time interval between AP upstrokes in response to the S1 and S2 stimuli at the S1S2 interval immediately preceding S2 refractoriness ($VERP_r$).

For the majority of experiments, in order to isolate measurements of VERP from the effects of conduction velocity, the heart was stimulated at the point of the recording electrode. The $VERP_s$ was used in these measurements as MAPs recorded close to the stimulus site unavoidably contained stimulus artefact and rendered the $VERP_r$ difficult to measure accurately. We thus consider our recording configuration to have achieved a situation similar to earlier studies that delivered S2 stimuli through the recording electrode and determined VERP from the upstroke of the last AP (rather than the S1 stimulus) to the upstroke resulting from the S2, which is usually synchronous with the S2 stimulus as they are at the same position [16].

In our final set of experiments, in order to investigate relationships between the VERP and the activation latency, we changed our protocol to pace at sites further from the recording electrode. In these experiments, the stimulating electrode and the epicardial LV and RV recording electrodes were clamped either 5 or 10 mm apart from each other. Endocardial MAPs could not be recorded in this way as the position of the endocardial electrodes within the ventricular cavity could not be fixed to this accuracy.

Care was taken to ensure that the stimulus potential applied was always kept at twice that of the threshold voltage to produce capture as stimulus intensity has a significant effect on VERP in itself [34]. The relationship between APD and VERP was calculated as the ratio between the two: VERP/APD. Transmural gradients of VERP were calculated as the difference (ΔVERP) between the endocardial and epicardial VERP values, i.e. (endocardial VERP) − (epicardial VERP), and transventricular gradients as the difference between RV and LV VERP values in the epicardium and endocardium.

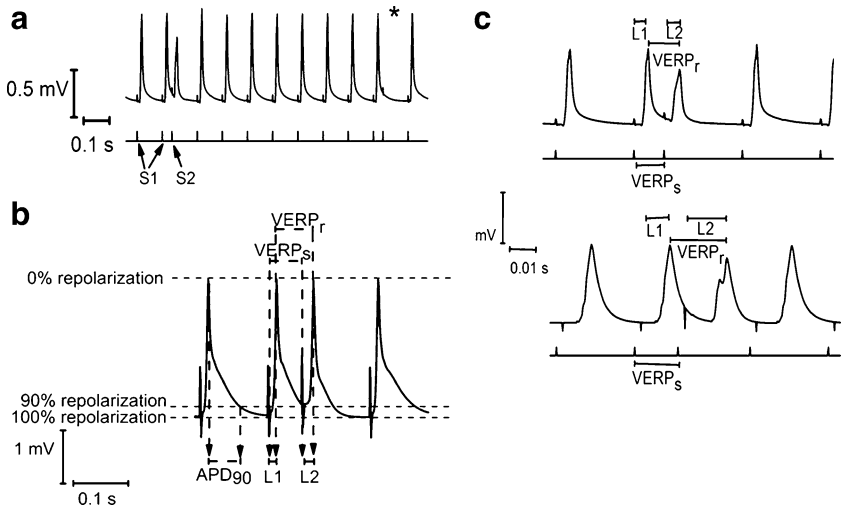

Fig. 1 Typical RV epicardial MAP recordings from a *Scn5a*$^{+/-}$ heart during the programmed stimulation (S1S2) protocol. **a** Recording showing the point of refractoriness (*asterisk*) where the S2 stimulus fails to elicit a response. The *equally spaced vertical markers below each trace* indicate S1 stimulus timings, with the *extra vertical markers* indicating S2 extra-stimuli. **b** Diagram illustrating measurement of: APD_{90}, L1 (latency following S1 stimulus), L2 (latency following S2 stimulus), $VERP_s$ (VERP at stimulus site) and the $VERP_r$ (VERP at recording site). **c** Recordings illustrating a situation in which the pacing and recording electrodes are adjacent (*top trace*) and a situation where the heart is paced from a site remote from the recording site (*bottom trace*). In the *top trace* $VERP_s$ and $VERP_r$ are 23 and 25 ms, respectively, whilst in the *bottom trace*, the $VERP_s$ is 24 ms and the $VERP_r$ is 53 ms

Twelve WT and 12 *Scn5a*$^{+/-}$ mice were used in all experiments, with half of each group eventually exposed to flecainide and half to quinidine. These results were expressed as mean±SEM values. Differences in activation latencies, APDs and VERPs, and gradients and ratios of the two, were analysed using ANOVA with post hoc Tukey's honestly significant different tests. Differences in arrhythmia incidences were analysed using Fisher's exact tests. Correlations between arrhythmia incidence and VERP gradients were analysed using Pearson's correlation. A p value of <0.05 was taken as a criterion for significance.

Results

VERP measurements are dependent upon the relationship between stimulus and recording site

As explained in "Materials and methods," the VERP was measured from the PES sequences. The VERP is traditionally measured as the shortest S1S2 time at which an S2 AP is recordable. It is therefore a function of the S1 and S2 stimulus times at the point of stimulation. However, for an AP to be detected by the recording electrode, the refractory period must have been exceeded throughout the tissue intervening between the sites of stimulation and recording. Thus, the VERP that is measured reflects the refractory time course in the entire line of tissue between the two. For this reason, the VERP is usually longer if pacing and stimulation are at different locations on the heart.

Previous studies in murine models have often adopted points of stimulation and recording on opposite, left and right, ventricles [42, 44]. This could account for previous reports of poor in vivo correlations between APD, measured at a single recording site by MAP catheter, and VERP, measured by a separate pacing catheter, that might reflect known variabilities of both APD and VERP between different ventricular sites, as well as differences in conduction velocity [16]. This issue led us to obtain two independent measures of VERP. Firstly, VERP at the stimulus site was determined from the S1S2 interval at which the S2 stimulus last excited an action potential ($VERP_s$). Second, VERP at the recording site was determined from the time interval between AP upstrokes in response to the S1 and S2 stimuli at the S1S2 interval immediately preceding S2 refractoriness ($VERP_r$).

However, if the stimulation and recording sites are far apart, the $VERP_r$ is further likely to be overestimated as the conduction velocity of the action potential resulting from the S2 stimulus is slowed as it passes through tissue in a relative refractory state, and therefore L2 is greater than L1. From Fig. 1c, we can see that:

$$VERP_r = VERP_s + (L2 - L1)$$

Therefore, we conducted measurements of both $VERP_s$ and $VERP_r$ at successively closer distances between stimulating and MAP recording electrodes. With decreasing interelectrode spacings, the $VERP_r$ reached a constant value in a given heart and converged with the $VERP_s$ to become statistically indistinguishable.

The increased arrhythmogenicity in Scn5a$^{+/-}$ hearts is accompanied by increased rather than decreased VERP

The programmed electrical stimulation procedures adopted here confirmed that *Scn5a*$^{+/-}$ hearts were more arrhythmogenic than WT (21% of traces vs. 6%, $p<0.01$, $n=12$) and that this tendency was increased by flecainide (to 40%, $p<0.01$, $n=6$) and decreased by quinidine (to 3%, $p<0.01$, $n=6$). This agreed with previous studies and established the phenotypic background against which subsequent findings could be compared [27, 44].

Figure 2 shows typical MAP recordings of the responses following the last S2 stimuli that elicited APs and from which APDs and VERPs could be calculated. The experiments confirmed previous studies [27] in which the APD was found to vary across regions of the heart so that the RV epicardial APD was shorter than the LV epicardial APD, and also shorter than the RV endocardial APD, thus setting up a significant repolarization gradient across the RV (Fig. 3a).

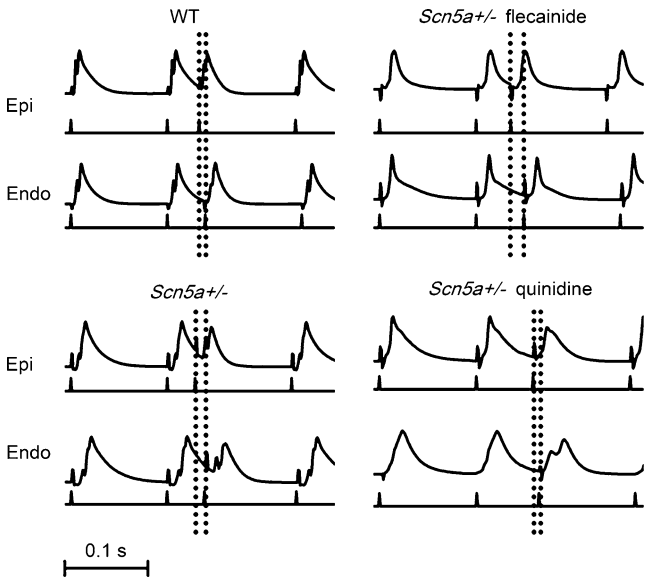

Fig. 2 Typical recordings from the RV epicardium and endocardium of a WT and a *Scn5a*$^{+/-}$ heart and from the *Scn5a*$^{+/-}$ heart after drug treatment. The part of the recording showing the last S2 in the programmed stimulation protocol which elicits an action potential is shown in each case. Recordings have been synchronized with respect to their S1 times to demonstrate the respective differences in VERPs (as calculated from S2 − S1). The *dotted vertical lines* denote the S2 timings of the epicardium followed by that of the endocardium and thus enable the difference between VERPs in the epicardium and endocardium in a given heart to be more easily compared

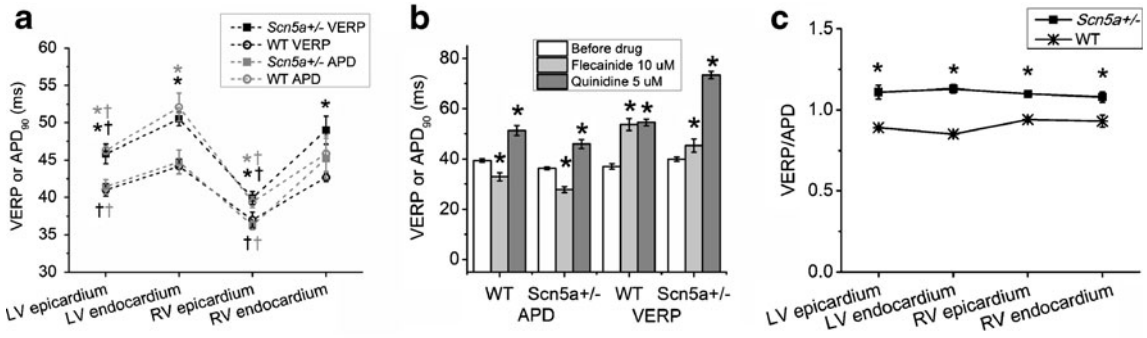

Fig. 3 **a** VERP and APD_{90} in four cardiac regions; $n=12$ for both WT and *Scn5a*$^{+/-}$. *Significant values of *t* tests between WT and *Scn5a*$^{+/-}$. †Significant values of *t* tests between cardiac regions within WT and *Scn5a*$^{+/-}$ hearts (*black*, VERP; *grey*, APD). **b** VERP and APD_{90} in the RV epicardium before and after drug exposure; $n=12$ prior to drug and $n=6$ in all cases following drug. *Significant values of *t* tests comparing values before and after drug administration (*black*, VERP; *grey*, APD). **c** VERP/APD_{90} in four cardiac regions; $n=12$ for both WT and *Scn5a*$^{+/-}$. *Significant values of *t* tests between WT and *Scn5a*$^{+/-}$

APDs of *Scn5a*$^{+/-}$ hearts were also shorter than the corresponding APDs of WT hearts, and were shortened by flecainide and lengthened by quinidine (Fig. 3b), in agreement with previous findings in murine [27] and pharmacological canine BrS models [20] as well as clinical studies [21].

However, measurements of VERPs taken from the same recordings were not in accord with predictions of reduced refractoriness required for early reentry phenomena. Instead, they related the *increased* arrhythmogenicity in *Scn5a*$^{+/-}$ with *increased*, rather than *decreased*, VERP and the pro- and anti-arrhythmic effects of flecainide and quinidine *both* with *increased* VERP. Firstly, despite the greater arrhythmogenicity in *Scn5a*$^{+/-}$ compared with WT, both variants showed similar patterns of shorter VERPs in the RV than the LV epicardium (39.9±0.9 vs. 45.8±1.3 ms, $p<0.05$, $n=12$ for *Scn5a*$^{+/-}$) and in the epicardium than the endocardium (39.9±0.9 vs. 49.9±1.9 ms, $p<0.05$, $n=12$ for RV in *Scn5a*$^{+/-}$; Fig. 3a). There were no endocardial transventricular VERP gradients.

Secondly, these variations paralleled the corresponding variations in APD, giving constant VERP/APD ratios through all the recording sites (Fig. 3c). This was in contrast to the greater arrhythmogenicity in the RV suggested in earlier studies. Thirdly, again in contrast to their *greater* arrhythmogenicity, *Scn5a*$^{+/-}$ hearts showed systematically *longer* VERPs than WT in all cardiac regions. Fourthly, the pro- and anti-arrhythmic agents flecainide and quinidine both *increased* VERPs in both WT and *Scn5a*$^{+/-}$ hearts in all regions, although the effect was more pronounced with quinidine than flecainide (e.g. 39.9±0.9 ms before drug to 45.3±2.6 ms with flecainide and to 73.3±1.5 ms with quinidine, $p<0.05$, $n=6$ for the RV in *Scn5a*$^{+/-}$; Fig. 3b). Finally, the larger VERP in the face of *smaller* APD values resulted in *larger* VERP/APD ratios in *Scn5a*$^{+/-}$ hearts than WT. All the mean VERP/APD values were <1 for the WT hearts, but were >1 for the *Scn5a*$^{+/-}$ hearts (e.g. 0.94±0.02 vs. 1.1±0.01, $p<0.05$, $n=12$ for the RV epicardium).

The increased arrhythmogenicity in Scn5a$^{+/-}$ hearts is accompanied by increased VERP gradients

Altered arrhythmogenicity, whether resulting from genetic or pharmacological manipulations, instead correlated with spatial variations in VERP. VERP gradients were explored using a strategy similar to previous explorations of APD gradients, as opposed to absolute APD values, between neighbouring ventricular regions [27] (Fig. 4a). Such differences are illustrated by comparing the MAP recordings in Fig. 2, which are synchronized to the timings of their S1 stimuli to demonstrate their respective VERP differences (as calculated from S2 − S1). The dotted vertical lines denote the timings of the S2 stimuli and demonstrate a greater transmural VERP gradient in *Scn5a*$^{+/-}$ than WT hearts. Flecainide increased both the mean VERP values and VERP gradients, whilst quinidine increased the mean values but decreased the VERP gradient.

The VERP gradients were greater across the RVs than the LVs in both *Scn5a*$^{+/-}$ and WT (e.g. 9.1±1.1 vs. 4.7±0.5 ms, $p<0.05$, $n=12$ for *Scn5a*$^{+/-}$). They were also greater in *Scn5a*$^{+/-}$ than WT hearts (e.g. 9.1±1.1 vs. 5.7±0.5 ms, $p<0.05$, $n=12$ for RV; Fig 4b). Furthermore, epicardial transventricular VERP gradients were greater in *Scn5a*$^{+/-}$ than WT (5.9±0.5 vs. 4.0±0.4 ms, $p<0.05$, $n=12$). Despite their respective pro- and anti-arrhythmic effects, treatment with either flecainide or quinidine did not affect ΔVERP values in the WT, apart from relatively small but still statistically significant increases in RV transmural gradient with flecainide (5.7±0.5 vs. 9.8±1.1 ms, $p<0.05$, $n=6$). In contrast, they exerted more noticeable effects particularly in the RV of *Scn5a*$^{+/-}$ hearts, where the ΔVERP was significantly increased (from 9.1±1.1 to 21±0.9 ms, $p<$

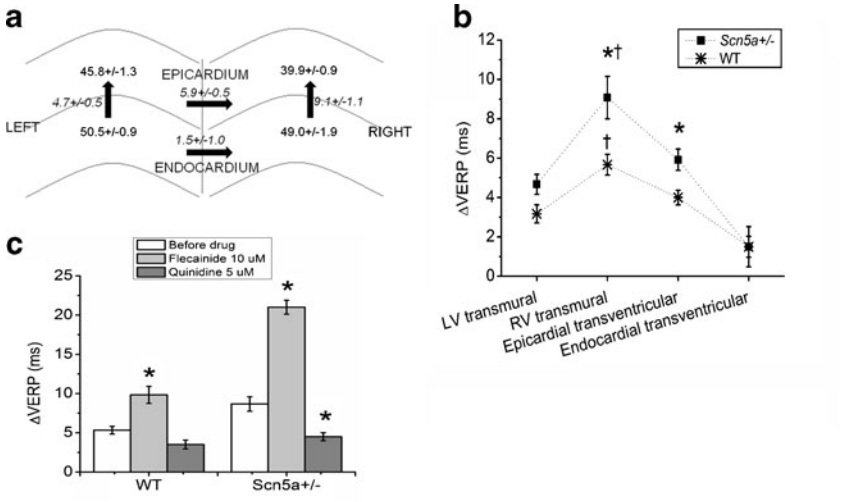

Fig. 4 **a** Four chambers of a typical *Scn5a*$^{+/-}$ heart are displayed diagrammatically: left and right epicardium and endocardium, with their respective VERP values in *normal font*. *Arrows* between the four areas depict the gradients between them, with ΔVERP values in *italic font*. Data are expressed as mean±SEM. **b** ΔVERP in four cardiac regions; $n=12$ for both WT and *Scn5a*$^{+/-}$. *Significant values of t tests between WT and *Scn5a*$^{+/-}$. †Significant values of t tests between cardiac regions within WT and *Scn5a*$^{+/-}$. **c** ΔVERP across the RV before and after exposure to flecainide or quinidine; $n=12$ prior to drug and $n=6$ in all cases following drug. *Significant values of t tests comparing values before and after drug administration

0.05, $n=6$) by flecainide and significantly decreased (to 4.5± 0.5 ms, $p<0.05$, $n=6$) by quinidine (Fig. 4c).

Such increases in VERP gradient correlated with increased arrhythmogenicity. Figure 5a shows a typical recording from the RV epicardium of a *Scn5a*$^{+/-}$ heart showing the initiation of VT by an S1S2 protocol. Figure 5b plots the values of RV transmural ΔAPD_{90} and ΔVERP against percentage incidences of arrhythmia recorded in both WT and *Scn5a*$^{+/-}$ hearts, before and after the addition of flecainide or quinidine. Linear fits can be constructed for both relationships, but ΔVERP has a very strong correlation with arrhythmogenic incidence, with a Pearson's coefficient of 0.970, whilst the coefficient for ΔAPD_{90} is only 0.731. Whilst these differences in correlation alone do not exclude a role for repolarization gradients in the ventricular arrhythmogenicity observed in BrS, they do support a scheme implicating regional differences in VERP rather than mean VERP values.

The increased VERPs in *Scn5a*$^{+/-}$ hearts are accompanied by increased latencies in activation by S2 stimuli

The final experiments correlated the increased VERPs in *Scn5a*$^{+/-}$ with increased slowing in the conduction following S2 stimuli, particularly following the addition of flecainide. The previous experiments, which had used closely placed pacing and recording electrodes, were modified by placing the electrodes on the same ventricle but spaced 5 or 10 mm apart. Activation latencies at a 0-mm interelectrode distance were all relatively short. Those

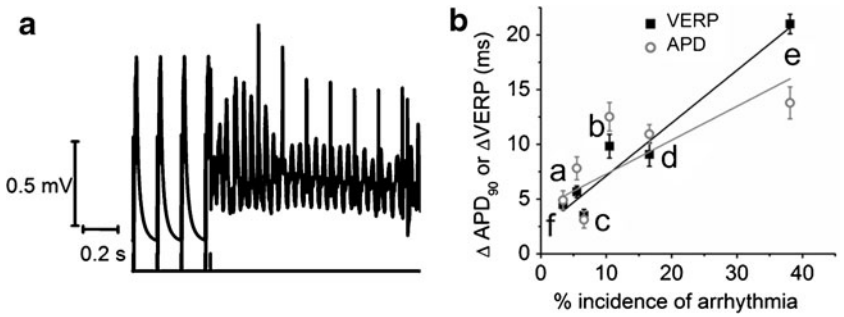

Fig. 5 **a** Example recording from the RV epicardium of a *Scn5a*$^{+/-}$ heart showing the initiation of VT during an S1S2 protocol. **b** Graph plotting RV transmural ΔAPD_{90} and ΔVERP against the percentage incidence of arrhythmia recorded in WT and *Scn5a*$^{+/-}$ hearts, before and after flecainide or quinidine. A strong positive correlation exists for ΔVERP (Pearson's correlation=0.970). *a* WT before drug, *b* WT after flecainide, *c* WT after quinidine, *d* *Scn5a*$^{+/-}$ before drug, *e* *Scn5a*$^{+/-}$ after flecainide, *f* *Scn5a*$^{+/-}$ after quinidine

in *Scn5a*$^{+/-}$ hearts were longer than those in WT hearts due to the slower AP depolarization, seen in a slower rise time of the MAP trace, as would be expected with a reduced number of activatable Na^+ channels. Recordings with the increased interelectrode spacings showed larger activation latencies as the distance through which the impulse had to travel was larger (Fig. 6a, b). They also showed greater differences between L2 and L1 (L2 − L1; Fig. 6c), as expected from the effects of slowed conduction through the partially refractory tissue, giving greater differences in $VERP_s$ and $VERP_r$, similar to the traces typified in Fig. 1c. However, whilst in all cases the differences between L2 and L1 increased as the interelectrode spacing increased, this effect was more pronounced in the *Scn5a*$^{+/-}$ hearts than in the WT hearts. Whilst the effect was similar between the LV and RV in the WT hearts, it was more pronounced in the RV than the LVof *Scn5a*$^{+/-}$ hearts. Flecainide and quinidine both slightly exacerbated the L2 − L1 increase with distance in WT hearts. However, in *Scn5a*$^{+/-}$ hearts, flecainide made the L2 − L1 increase very much more markedly with distance, whilst this effect was attenuated by quinidine. These final experiments thus suggest a scheme in which variations in VERP can act to produce arrhythmias through alterations in conduction velocity.

Discussion

The present studies examining VERPs and conduction latencies follow from recent findings of increased RV transmural APD gradients in *Scn5a*$^{+/-}$ hearts [27], which might predispose the epicardium to early, phase II, re-excitation. The occurrence of these early re-excitation phenomena suggested for BrS would require correspondingly early recoveries from refractoriness. On the other hand, they would be excluded by a combination of *shortened* APDs but *lengthened* VERPs. The present experiments test these possibilities for the first time.

WT and *Scn5a*$^{+/-}$ hearts both showed regional heterogeneities in VERPs, consistent with both clinical reports [23] and known differences in outward I_{to} potassium current [13, 45]. However, comparisons between WT and *Scn5a*$^{+/-}$ hearts revealed contrasting rather than concordant APD and VERP differences and associated the arrhythmogenic *Scn5a*$^{+/-}$ phenotype with greater rather than reduced VERPs. Whilst these findings may seem surprising, they are consistent with expectations from reduced numbers of Na^+ channels available for re-excitation in *Scn5a*$^{+/-}$ hearts. The duration of refractoriness is dependent upon a recovery of a critical number of activatable Na^+ channels. A greater relative proportion of such channels would then be required to enable resumption of excitability, and this would occur later in the repolarization phase. This hypothesis is consistent with the present findings following Na^+ reduction by genetic means in *Scn5a*$^{+/-}$ hearts or by pharmacological means through the effects of Na^+ channel blockers. Previous computational studies modelling situations of reduced Na^+ conductance [40, 43], as well as experimental studies showing reduced Na^+ conductance in ischaemic tissue [39], have also demonstrated increased refractory periods.

The pro- and anti-arrhythmic agents flecainide and quinidine *both increased* regional VERPs. The effect was more pronounced with quinidine than with flecainide, probably due to the additional strong K^+ channel-blocking actions of quinidine, as opposed to flecainide whose predominant effect is on Na^+ channels without a significant effect on K^+ channels [50]. However, the action of both drugs in increasing VERP is consistent with their known effects in canine and rabbit preparations [8, 17], as well as human hearts [36, 41]. Together, these findings associated *increased* arrhythmogenicity in *Scn5a*$^{+/-}$ hearts with a combination of *shortened* APDs but *increased* VERP. This is in agreement with observations in isolated porcine hearts in which flecainide exerted anti-arrhythmogenic properties in tissue with short VERPs but pro-arrhythmic effects in tissue

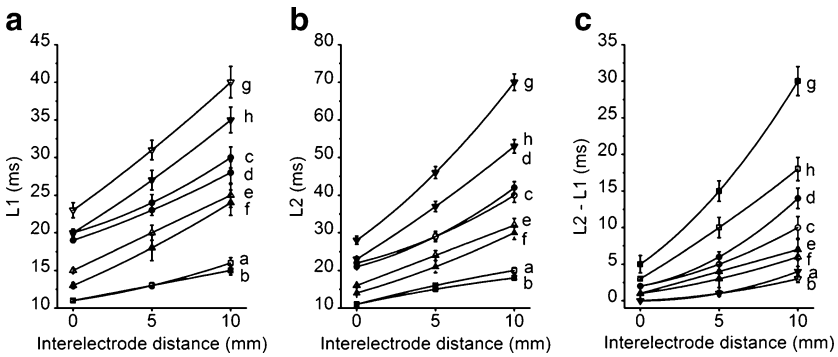

Fig. 6 Graph of epicardial L1 (**a**) and L2 (**b**) and the time difference between L2 and L1 (**c**) against the interelectrode distance. A second-order polynomial is fitted to each relationship. *a* LV WT before drug, *b* RV WT before drug, *c* LV *Scn5a*$^{+/-}$ before drug, *d* RV *Scn5a*$^{+/-}$ before drug, *e* RV WT after flecainide, *f* RV WT after quinidine, *g* RV *Scn5a*$^{+/-}$ after flecainide, *h* RV *Scn5a*$^{+/-}$ after quinidine

with longer VERPs [9]. However, all these findings directly conflict with a more established hypothesis, first proposed following experiments in the canine pharmacological wedge preparation where electrotonic forces between sites at which the APD is maintained and those at which it is attenuated due to loss of the AP dome can produce an extrasystole via local re-excitation (phase 2 reentry), which in turn can initiate circus movement reentry [51]. Whilst studies in the *Scn5a*$^{+/-}$ mice have indeed shown increased repolarization gradients in the RV [27], this proposed mechanism of early re-excitation would require shortened VERPs to allow reentrant circuits to flow and therefore would be unlikely to occur in the situation of increased refractoriness seen in our study.

However, the findings remain compatible with an important role of refractory periods, in particular their spatial variations and the consequences of these for conduction, in the initiation of reentrant arrhythmia in BrS. We have shown a strong correlation between refractory gradients and arrhythmia incidence in the *Scn5a*$^{+/-}$ mice. This study cannot itself prove a causal link between the two or demonstrate the underlying molecular mechanism; however, similar arrhythmogenic effects of increased VERP dispersion have been observed elsewhere in experiments in genetic and pharmacological animal models of long QT syndrome [3, 18], short QT syndrome [31] and ischemia [19, 33], as well as modelling studies [47]. Similarly, patients with long QT syndrome [49] and arrhythmic post-infarct patients [32] also show greater dispersions of refractory periods. Here, *Scn5a*$^{+/-}$ hearts showed greater VERP gradients than WT, particularly across the RV, compatible with differences in the sensitivity of membrane potentials in areas of different K^+ current density. *Scn5a*$^{+/-}$ hearts also showed greater conduction slowing than WT hearts following S2 stimuli, particularly following flecainide treatment, in line with clinical findings [37]. Whilst quinidine also increased the latencies both following S1 and S2 stimuli, it did so to a lesser extent than flecainide, in particular for L2. This is again likely to be due to the relatively dominant effects of flecainide on the Na^+ channel, as opposed to quinidine's stronger action on the K^+ channel. Thus, whilst quinidine may have a larger effect in increasing the refractory period itself, flecainide's actions in Na^+ channel blockade leads to greater conduction slowing and thus heterogeneity in tissue excitability and refractoriness [50]. As well as being generated by refractory heterogeneity, conduction slowing can also occur directly as a result of Na^+ channel dysfunction and resulting reduction in AP depolarization velocity [48], which can add to the likelihood of reentrant circuits being formed. It is furthermore possible that the heterogeneities in our model are increased by the presence of areas of local fibrosis, particularly in the RV, as documented both in clinical cases of BrS [10] and in the *Scn5a*$^{+/-}$ mouse model [48].

This study adds to a recent series of papers by our group attempting to elucidate the mechanisms of arrhythmogenesis using a murine model of BrS. We have previously demonstrated both depolarization abnormalities, in the form of delayed conduction latencies [27] and slowed activation patterns [25], and repolarization abnormalities, in the form of heterogeneities in APDs and steep restitution curves with high incidences of discordant alternans [24]. However, the evidence in the present studies links these two mechanisms by correlating the arrhythmic propensity shown by *Scn5a*$^{+/-}$ hearts with reentrant arrhythmias attributable to enhanced RV transmural refractory gradients, in turn leading to slowed conduction. Our 'loss-of-function' *Scn5a*$^{+/-}$ hearts show a 50% reduction in the early transmembrane Na^+ current [35] that reduces the speed and amplitude of the depolarization wave. Impulse propagation from S2 stimuli is further reduced as the impulse travels through partially refractory tissue. In situations of prolonged refractoriness, impulses are increasingly likely to travel through tissue which is still partially refractory. Therefore, heterogeneity in tissue excitability of itself can promote tachycardias as a result of slowed conduction and functional conduction block, leading to wave breakup and reentrant excitation.

Our study could also be helpful in elucidating the role of the ST elevation in the right precordial leads that is characteristic of BrS and that is also seen in the *Scn5a*$^{+/-}$ mice [26]. Opinion is currently divided as to whether the ST elevation is caused by depression or loss of action potential dome in the RV epicardium, creating a transmural voltage gradient [1], or through a selectively slowed conduction at the RVOT [37]. The mechanisms underlying the ST elevation and the ventricular arrhythmogenesis are generally assumed to be linked, particularly as both phenomena are localized to the RV and in light of observations of accentuated ST elevation immediately preceding VF [28]. However, it is possible that whilst transmural voltage gradients cause the ST elevation, it is in fact associated with changes in refractory properties of the tissue, and hence conduction slowing, which then leads to the initiation of reentrant circuits.

The main limitations of the study are associated with the use of a mouse model. Our model is a heterozygote for the *Scn5a* gene, and we are therefore limited in investigating the role of other voltage-gated ion channels, in particular voltage-gated Ca^{2+} channels, which could also play a role in triggering cardiac events in BrS patients. Secondly, the small size of the mouse heart means that strong electrotonic forces may act to minimize the effect of any spatial heterogeneities that are created and reduce their potential to create a reentrant substrate. The action potential morphology differs between humans and mice as mice use less L-type Ca^{2+} channel current, which means that the mouse AP does not have a plateau phase and has a shorter

APD [11]. This means that the spike and dome morphology present in larger mammals is not present in our mouse model. However, we were able to demonstrate a clear propensity to arrhythmia in our BrS mouse model and correlate this with enhanced RV transmural refractory gradients despite these limitations.

Acknowledgements Funding was provided by the British Heart Foundation, the Medical Research Council, the Wellcome Trust and the Biotechnology and Biological Research Council, UK. CAM was supported by a Medical Research Council Clinical Research Fellowship and a Sackler Studentship of the University of Cambridge School of Clinical Medicine.

Ethical standards All procedures, including sacrificing by schedule 1, conformed to the UK Animals (Scientific Procedures) Act 1986. Experiments were performed under personal and project licences (PIL 80/1243 and PPL 80/1974) approved by local ethical committees and issued by the UK Home Office.

Conflict of interest The authors have no conflicts of interest.

Open Access This article is distributed under the terms of the Creative Commons Attribution Noncommercial License which permits any noncommercial use, distribution, and reproduction in any medium, provided the original author(s) and source are credited.

References

1. Antzelevitch C (2001) The Brugada syndrome: ionic basis and arrhythmia mechanisms. J Cardiovasc Electrophysiol 12:268–272
2. Ashino S, Watanabe I, Kofune M et al (2010) Abnormal action potential duration restitution property in the right ventricular outflow tract in Brugada syndrome. Circ J 74:664–670
3. Baker LC, London B, Choi BR, Koren G, Salama G (2000) Enhanced dispersion of repolarization and refractoriness in transgenic mouse hearts promotes reentrant ventricular tachycardia. Circ Res 86:396–407
4. Balasubramaniam R, Grace AA, Saumarez RC, Vandenberg JI, Huang CL (2003) Electrogram prolongation and nifedipine-suppressible ventricular arrhythmias in mice following targeted disruption of KCNE1. J Physiol 552:535–546
5. Belhassen B, Glick A, Viskin S (2004) Efficacy of quinidine in high-risk patients with Brugada syndrome. Circulation 110:1731–1737
6. Bezzina CR, Rook MB, Wilde AA (2001) Cardiac sodium channel and inherited arrhythmia syndromes. Cardiovasc Res 49:257–271
7. Brugada R, Brugada J, Antzelevitch C, Kirsch GE, Potenza D, Towbin JA, Brugada P (2000) Sodium channel blockers identify risk for sudden death in patients with ST-segment elevation and right bundle branch block but structurally normal hearts. Circulation 101:510–515
8. Brugada J, Sassine A, Escande D, Masse C, Puech P (1987) Effects of quinidine on ventricular repolarization. Eur Heart J 8:1340–1345
9. Coronel R, Wilms-Schopman FJG, Janse MJ (2010) Anti- or profibrillatory effects of Na^+ channel blockade depend on the site of application relative to gradients in repolarization. Front. Physio 1:10
10. Coronel R, Casini S, Koopmann TT, Wilms-Schopman FJ, Verkerk AO, de Groot JR, Bhuiyan Z, Bezzina CR, Veldkamp MW, Linnenbank AC, van der Wal AC, Tan HL, Brugada P, Wilde AA, de Bakker JM (2005) Right ventricular fibrosis and conduction delay in a patient with clinical signs of Brugada syndrome: a combined electrophysiological, genetic, histopathologic, and computational study. Circulation 112:2769–2777
11. Danik S, Cabo C, Chiello C, Kang S, Wit AL, Coromilas J (2002) Correlation of repolarization of ventricular monophasic action potential with ECG in the murine heart. Am J Physiol Heart Circ Physiol 283:H372–H381
12. Davidenko JM, Antzelevitch C (1986) Electrophysiological mechanisms underlying rate-dependent changes of refractoriness in normal and segmentally depressed canine Purkinje fibers. The characteristics of post-repolarization refractoriness. Circ Res 58:257–268
13. Di Diego JM, Sun ZQ, Antzelevitch C (1996) *I*(to) and action potential notch are smaller in left vs. right canine ventricular epicardium. Am J Physiol 271:H548–H561
14. Eckardt L, Probst V, Smits JP, Bahr ES, Wolpert C, Schimpf R, Wichter T, Boisseau P, Heinecke A, Breithardt G, Borggrefe M, LeMarec H, Bocker D, Wilde AA (2005) Long-term prognosis of individuals with right precordial ST-segment-elevation Brugada syndrome. Circulation 111:257–263
15. Franz MR, Chin MC, Sharkey HR, Griffin JC, Scheinman MM (1990) A new single catheter technique for simultaneous measurement of action potential duration and refractory period in vivo. J Am Coll Cardiol 16:878–886
16. Franz MR, Costard A (1988) Frequency-dependent effects of quinidine on the relationship between action potential duration and refractoriness in the canine heart in situ. Circulation 77:1177–1184
17. Ikeda N, Singh BN, Davis LD, Hauswirth O (1985) Effects of flecainide on the electrophysiologic properties of isolated canine and rabbit myocardial fibers. J Am Coll Cardiol 5:303–310
18. Inoue H, Toda I, Nozaki A, Matsuo H, Mashima S, Sugimoto T (1985) Inhomogeneity of ventricular refractory period in canine heart with quinidine-induced long QT interval: a comparative study on effects of heart rate, isoprenaline, and lignocaine. Cardiovasc Res 19:623–630
19. Isomura S, Ando S, Kobe T, Ohta T, Toyama J, Yamada K (1981) Dispersion of effective refractory period in the ischemic border zone in canine heart. Jpn Circ J 45:905–906
20. Krishnan SC, Antzelevitch C (1991) Sodium channel block produces opposite electrophysiological effects in canine ventricular epicardium and endocardium. Circ Res 69:277–291
21. Kurita T, Shimizu W, Inagaki M, Suyama K, Taguchi A, Satomi K, Aihara N, Kamakura S, Kobayashi J, Kosakai Y (2002) The electrophysiologic mechanism of ST-segment elevation in Brugada syndrome. J Am Coll Cardiol 40:330–334
22. Lee RJ, Liem LB, Cohen TJ, Franz MR (1992) Relation between repolarization and refractoriness in the human ventricle: cycle length dependence and effect of procainamide. J Am Coll Cardiol 19:614–618
23. Luo J, Pripp CM, Hertervig E, Kongstad O, Ljungstrom E, Olsson SB, Yuan S (2004) Non-invasive evaluation of ventricular refractoriness and its dispersion during ventricular fibrillation in patients with implantable cardioverter defibrillator. BMC Cardiovasc Disord 4:8
24. Martin CA, Grace AA, Huang CL (2011) Spatial and temporal heterogeneities are localized to the right ventricular outflow tract in a heterozygotic *Scn5a* mouse model. Am J Physiol Heart Circ Physiol 300:H605–H616
25. Martin CA, Guzadhur L, Grace AA, Lei M, Huang CL (2011) Mapping of reentrant spontaneous polymorphic ventricular tachycardia in a *Scn5a*$^{+/-}$ mouse model. Am J Physiol Heart Circ Physiol 300: H1853–H1862

26. Martin CA, Zhang Y, Grace AA, Huang CL (2010) In vivo studies of *Scn5a*$^{+/-}$ mice modeling Brugada syndrome demonstrate both conduction and repolarization abnormalities. J Electrocardiol 43:433–439
27. Martin CA, Zhang Y, Grace AA, Huang CL (2010) Increased right ventricular repolarization gradients promote arrhythmogenesis in a murine model of Brugada syndrome. J Cardiovasc Electrophysiol 21:1153–1159
28. Matsuo K, Shimizu W, Kurita T, Inagaki M, Aihara N, Kamakura S (1998) Dynamic changes of 12-lead electrocardiograms in a patient with Brugada syndrome. J Cardiovasc Electrophysiol 9:508–512
29. Matthews GD, Martin CA, Grace AA, Zhang Y, Huang CL (2010) Regional variations in action potential alternans in isolated murine *Scn5a*(+/−) hearts during dynamic pacing. Acta Physiol (Oxf) 2:129–146
30. Meregalli PG, Wilde AA, Tan HL (2005) Pathophysiological mechanisms of Brugada syndrome: depolarization disorder, repolarization disorder, or more? Cardiovasc Res 67:367–378
31. Milberg P, Tegelkamp R, Osada N, Schimpf R, Wolpert C, Breithardt G, Borggrefe M, Eckardt L (2007) Reduction of dispersion of repolarization and prolongation of postrepolarization refractoriness explain the antiarrhythmic effects of quinidine in a model of short QT syndrome. J Cardiovasc Electrophysiol 18:658–664
32. Misier AR, Opthof T, van Hemel NM, Vermeulen JT, de Bakker JM, Defauw JJ, van Capelle FJ, Janse MJ (1995) Dispersion of 'refractoriness' in noninfarcted myocardium of patients with ventricular tachycardia or ventricular fibrillation after myocardial infarction. Circulation 91:2566–2572
33. Naimi S, Avitall B, Mieszala J, Levine HJ (1977) Dispersion of effective refractory period during abrupt reperfusion of ischemic myocardium in dogs. Am J Cardiol 39:407–412
34. Opthof T, Coronel R, Vermeulen JT, Verberne HJ, van Capelle FJ, Janse MJ (1993) Dispersion of refractoriness in normal and ischaemic canine ventricle: effects of sympathetic stimulation. Cardiovasc Res 27:1954–1960
35. Papadatos GA, Wallerstein PM, Head CE, Ratcliff R, Brady PA, Benndorf K, Saumarez RC, Trezise AE, Huang CL, Vandenberg JI, Colledge WH, Grace AA (2002) Slowed conduction and ventricular tachycardia after targeted disruption of the cardiac sodium channel gene *Scn5a*. Proc Natl Acad Sci USA 99:6210–6215
36. Platia EV, Estes M, Heine DL, Griffith LS, Garan H, Ruskin JN, Reid PR (1985) Flecainide: electrophysiologic and antiarrhythmic properties in refractory ventricular tachycardia. Am J Cardiol 55:956–962
37. Postema PG, van Dessel PFHM, de Bakker JMT, Dekker LRC, Linnenbank AC, Hoogendijk MG, Coronel R, Tijssen JGP, Wilde AAM, Tan HL (2008) Slow and discontinuous conduction conspire in Brugada syndrome: a right ventricular mapping and stimulation study. Circ Arrhythmia Electrophysiol 1:379–386
38. Postema PG, Wolpert C, Amin AS, Probst V, Borggrefe M, Roden DM, Priori SG, Tan HL, Hiraoka M, Brugada J, Wilde AA (2009) Drugs and Brugada syndrome patients: review of the literature, recommendations, and an up-to-date website (www.brugadadrugs.org). Heart Rhythm 6:1335–1341
39. Pu J, Boyden PA (1997) Alterations of Na^+ currents in myocytes from epicardial border zone of the infarcted heart. A possible ionic mechanism for reduced excitability and postrepolarization refractoriness. Circ Res 81:110–119
40. Qu Z, Karagueuzian HS, Garfinkel A, Weiss JN (2004) Effects of Na(+) channel and cell coupling abnormalities on vulnerability to reentry: a simulation study. Am J Physiol Heart Circ Physiol 286: H1310–H1321
41. Rosenheck S, Schmaltz S, Kadish AH, Summitt J, Morady F (1991) The effect of quinidine and mexiletine on the adaptation of ventricular refractoriness to an increase in rate. Am Heart J 121:512–517
42. Sabir IN, Fraser JA, Killeen MJ, Grace AA, Huang CL (2007) The contribution of refractoriness to arrhythmic substrate in hypokalemic Langendorff-perfused murine hearts. Pflugers Arch 454:209–222
43. Starmer CF, Colatsky TJ, Grant AO (2003) What happens when cardiac Na channels lose their function? 1—Numerical studies of the vulnerable period in tissue expressing mutant channels. Cardiovasc Res 57:82–91
44. Stokoe KS, Balasubramaniam R, Goddard CA, Colledge WH, Grace AA, Huang CL (2007) Effects of flecainide and quinidine on arrhythmogenic properties of *Scn5a*$^{+/-}$ murine hearts modelling the Brugada syndrome. J Physiol 581:255–275
45. Teutsch C, Kondo RP, Dederko DA, Chrast J, Chien KR, Giles WR (2007) Spatial distributions of Kv4 channels and KChip2 isoforms in the murine heart based on laser capture microdissection. Cardiovasc Res 73:739–749
46. Theisen K, Vogler A, Kotzur J (1984) Effect of pacing duration on right ventricular effective refractory period in man. Klin Wochenschr 62:773–776
47. Trenor B, Romero L, Ferrero J, Saiz J, Molto G, Hernandez V (2007) Dispersion of refractoriness in a simulated ischemic 2D tissue and implications in vulnerability to reentry. Proceedings of Computers in Cardiology, Durham, North Carolina
48. van Veen TA, Stein M, Royer A, Le Quang K, Charpentier F, Colledge WH, Huang CL, Wilders R, Grace AA, Escande D, de Bakker JM, van Rijen HV (2005) Impaired impulse propagation in *Scn5a*-knockout mice: combined contribution of excitability, connexin expression, and tissue architecture in relation to aging. Circulation 112:1927–1935
49. Vassallo JA, Cassidy DM, Kindwall KE, Marchlinski FE, Josephson ME (1988) Nonuniform recovery of excitability in the left ventricle. Circulation 78:1365–1372
50. Wang ZG, Pelletier LC, Talajic M, Nattel S (1990) Effects of flecainide and quinidine on human atrial action potentials. Role of rate-dependence and comparison with guinea pig, rabbit, and dog tissues. Circulation 82:274–283
51. Yan GX, Antzelevitch C (1999) Cellular basis for the Brugada syndrome and other mechanisms of arrhythmogenesis associated with ST-segment elevation. Circulation 100:1660–1666